Supplementary Figures

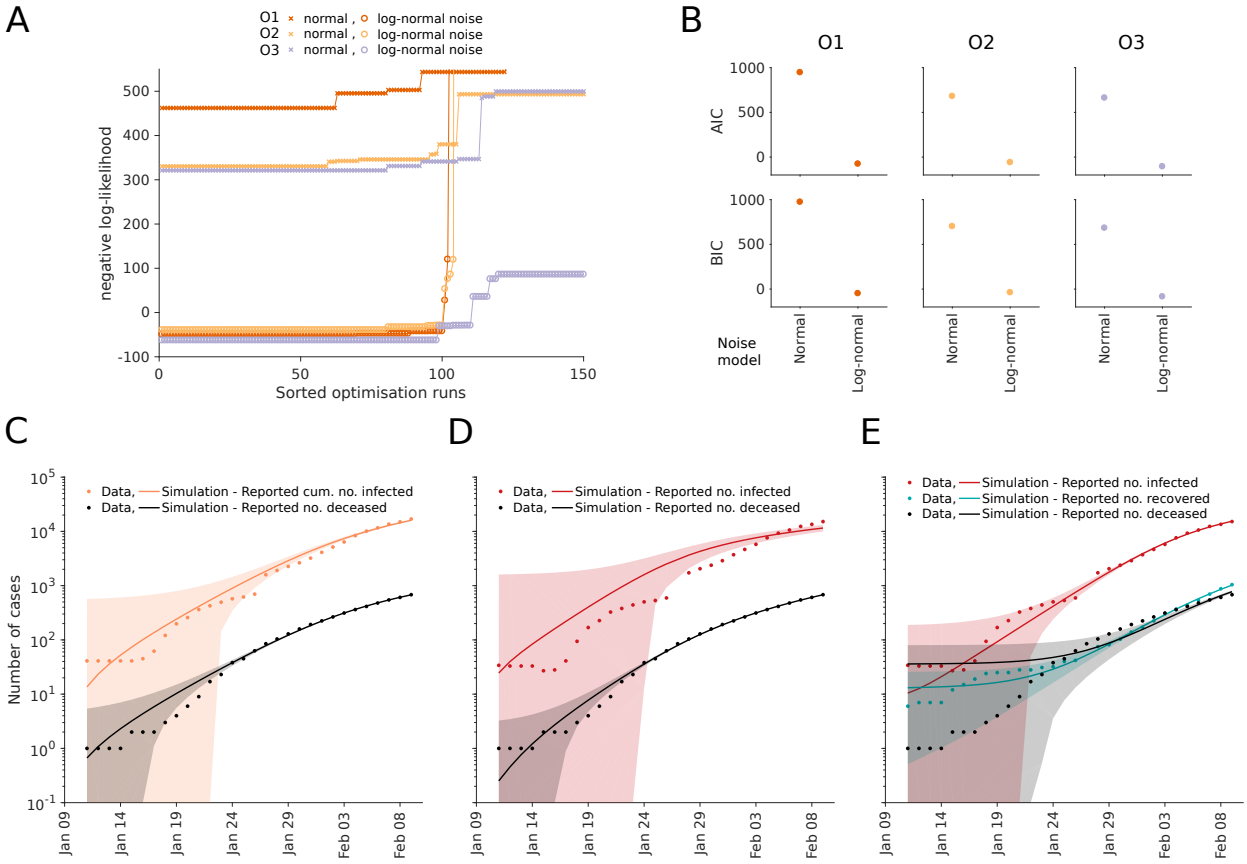

Figure S1: **Optimisation and model selection results for observable and noise model comparison.** (A) Waterfall plots for the best 150 out of 200 multi-start runs. The optimisation runs are sorted by increasing negative log-likelihood value. (B) AIC and BIC values. (C,D,E) Fitting results for observation scenarios O1, O2, and O3 assuming normally distributed noise. The simulation for the maximum likelihood estimate (line) and interval for +/− one standard deviation of the inferred noise level (shaded area) is depicted.

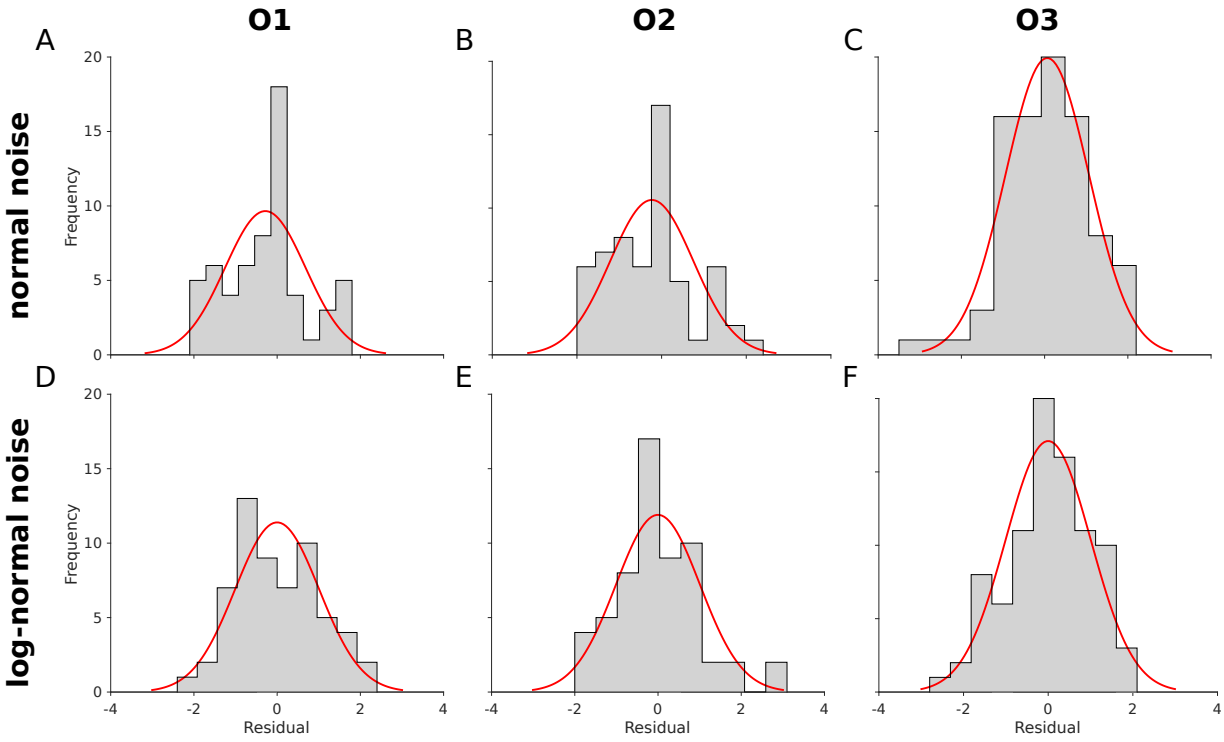

Figure S2: **Evaluation of residual distributions.** (A-C) Distributions of the residuals $(\bar{y}_{i,k} - y_i(t_k))/\sigma_i$ for all observables and time points under the assumption of normally distributed measurement noise. (D-F) Distributions of the residuals $(\log \bar{y}_{i,k} - \log y_i(t_k))/\sigma_i$ for all observables and time points under the assumption of log-normally distributed measurement noise. The different columns contain the information for the fitting scenarios O1 to O3. The histogram indicates the empirical frequency of observations and the red line the theoretical limit distribution.

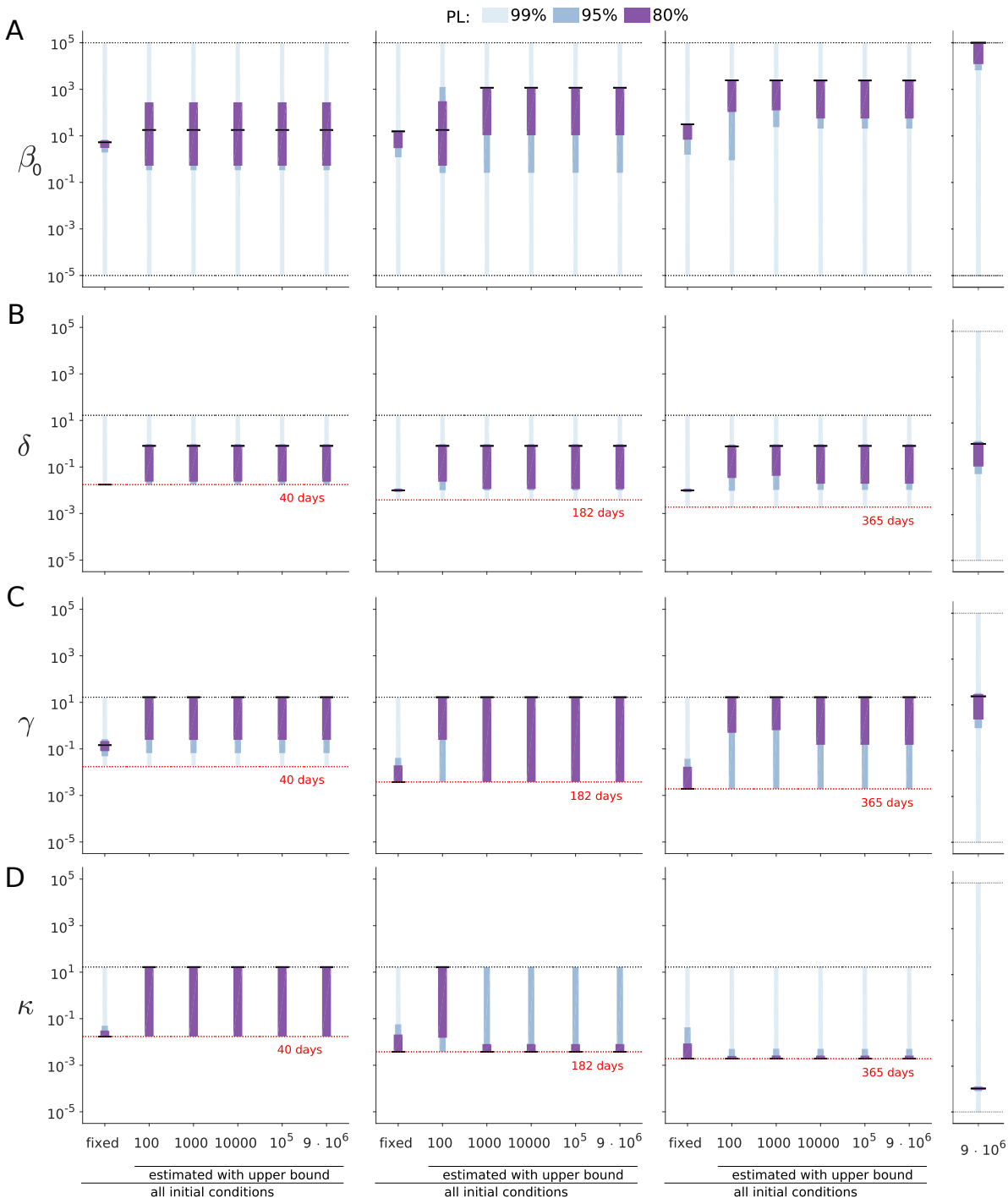

Figure S3: **Analysis of the impact of different bounds for rate constants and initial conditions on the parameter estimations and their uncertainties for model O1.** The profile likelihood-based confidence intervals are depicted for (A) the transmission rate β_0, (B) the death rate δ, (C) the recovery rate γ, and (D) the progression rate κ. An upper bound for the inverse of each rate constant was set to 40 days (left), 182 days (middle), and 365 days (right). The plots on the far right depict the most conservative setting with boundaries from 10^{-5} to 10^5. The different upper bounds for the initial conditions are depicted on the x-axis.

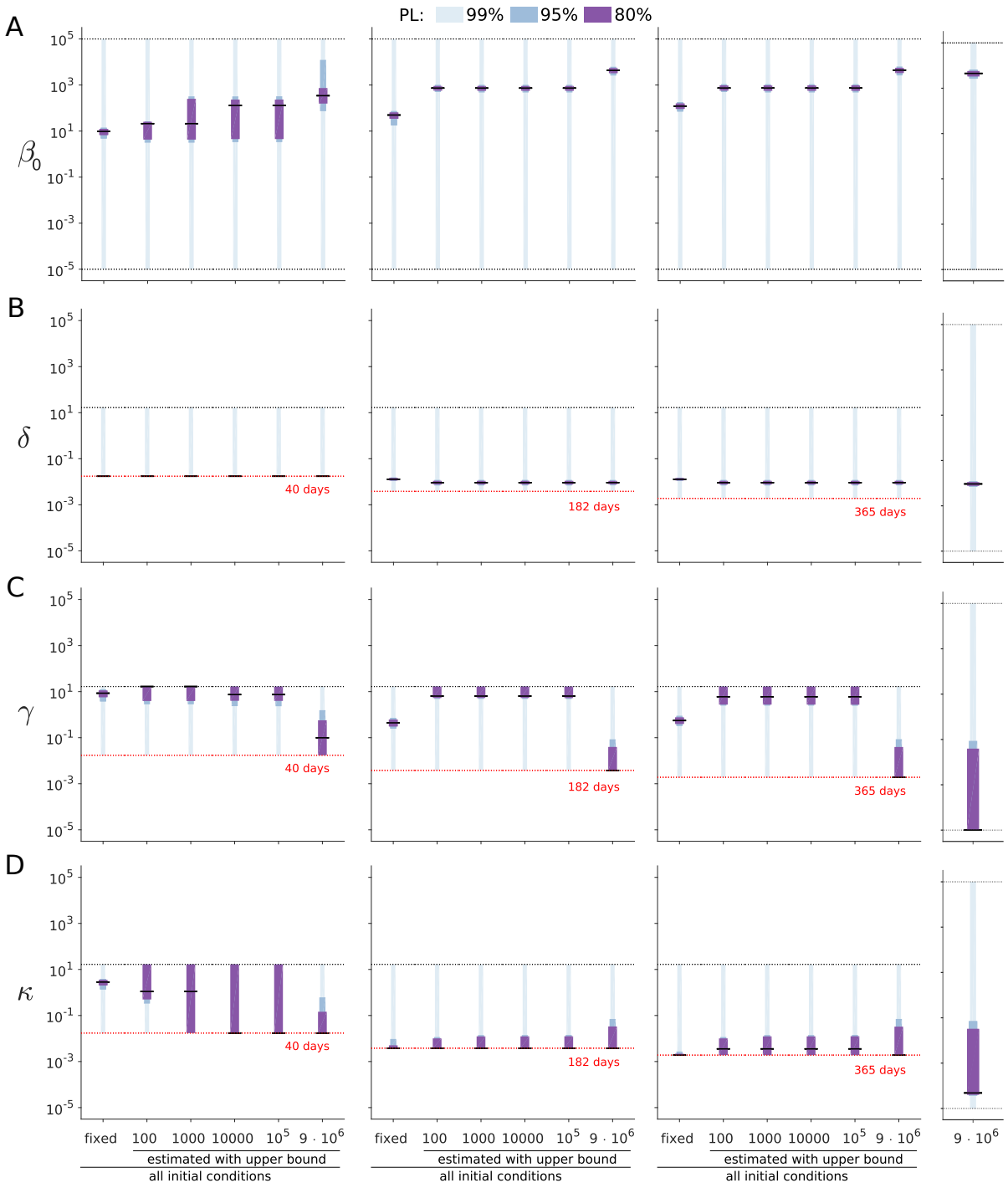

Figure S4: **Analysis of the impact of different bounds for rate constants and initial conditions on the parameter estimations and their uncertainties for model O2.** The profile likelihood-based confidence intervals are depicted for (A) the transmission rate β_0, (B) the death rate δ, (C) the recovery rate γ, and (D) the progression rate κ. An upper bound for the inverse of each rate constant was set to 40 days (left), 182 days (middle), and 365 days (right). The plots on the far right depict the most conservative setting with boundaries from 10^{-5} to 10^5. The different upper bounds for the initial conditions are depicted on the x-axis.

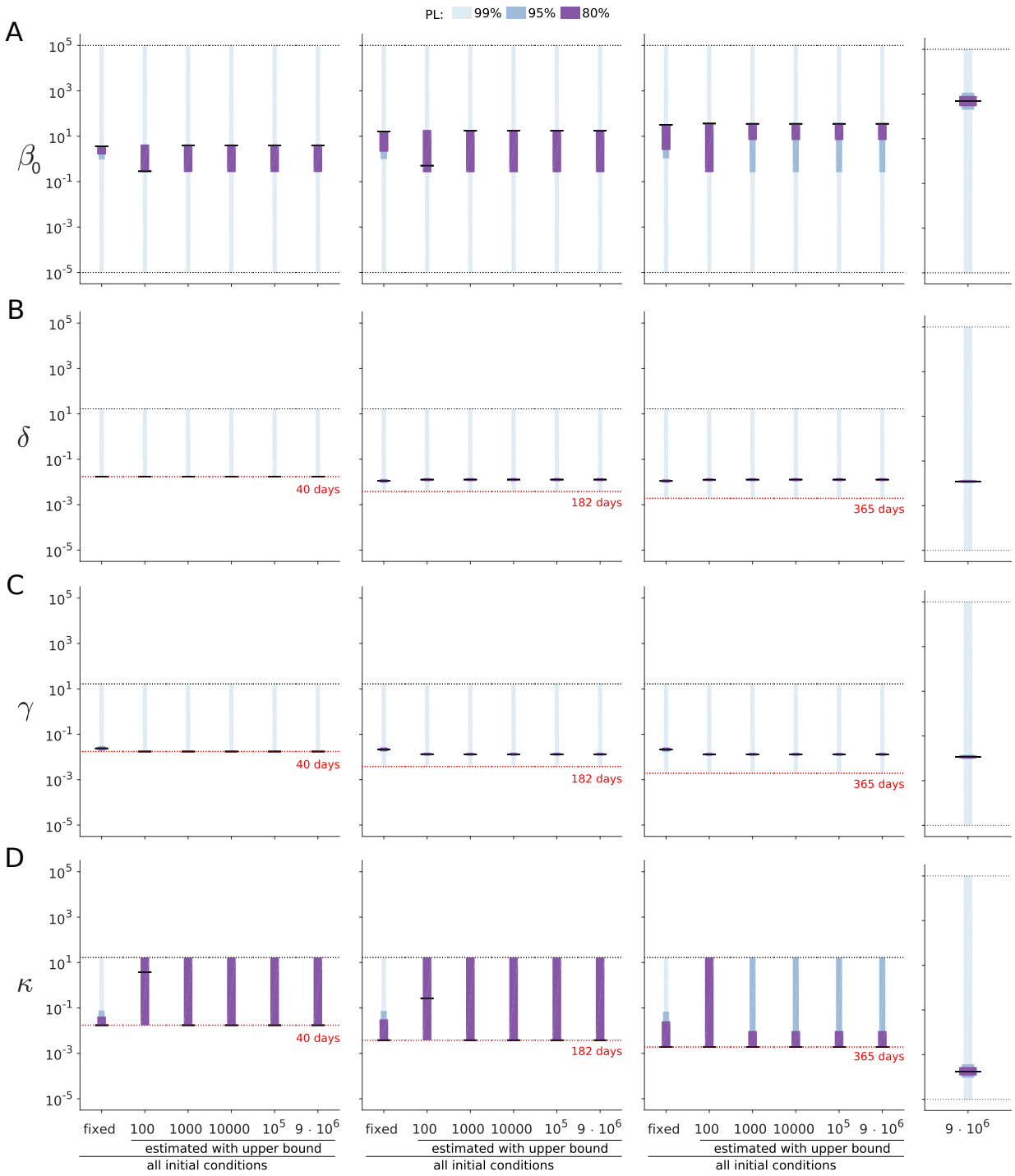

Figure S5: **Analysis of the impact of different bounds for rate constants and initial conditions on the parameter estimations and their uncertainties for model O3.** The profile likelihood-based confidence intervals are depicted for (A) the transmission rate β_0, (B) the death rate δ, (C) the recovery rate γ, and (D) the progression rate κ. An upper bound for the inverse of each rate constant was set to 40 days (left), 182 days (middle), and 365 days (right). The plots on the far right depict the most conservative setting with boundaries from 10^{-5} to 10^5. The different upper bounds for the initial conditions are depicted on the x-axis.

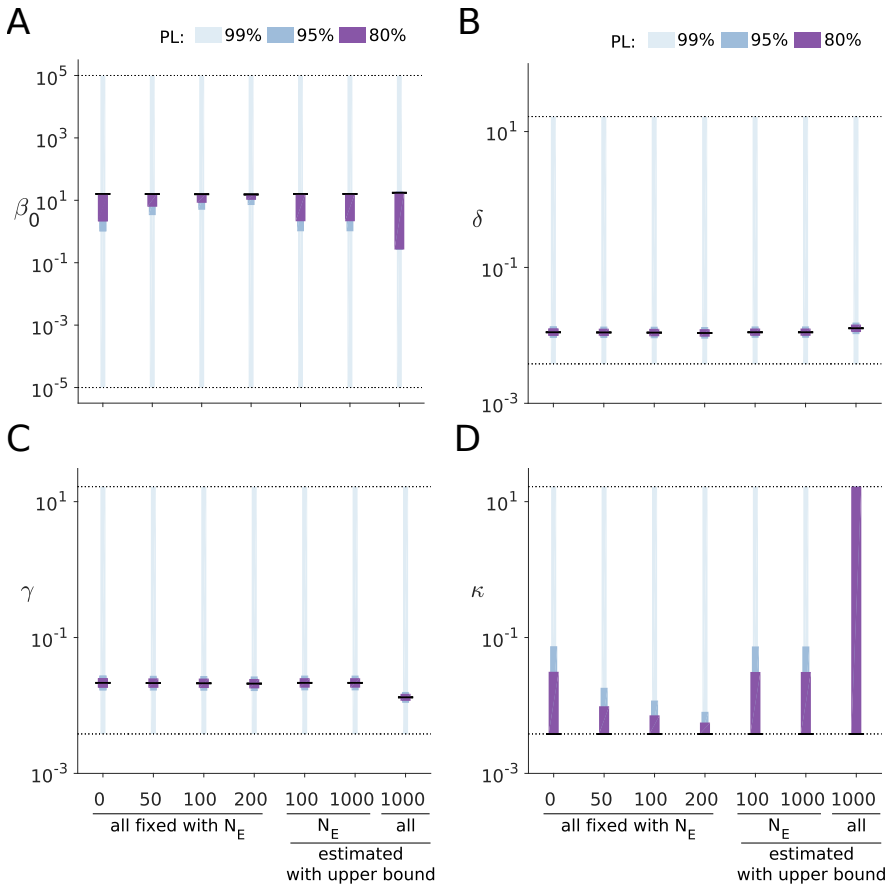

Figure S6: **Analysis of the impact of fixing or estimating initial exposed individuals (N_E) on the parameter uncertainties for model O3.** The profile likelihood-based confidence intervals are depicted for (A) the transmission rate β_0, (B) the death rate δ, (C) the recovery rate γ, and (D) the progression rate κ. An upper bound for the inverse of the rate constants was set for all to 182 days.

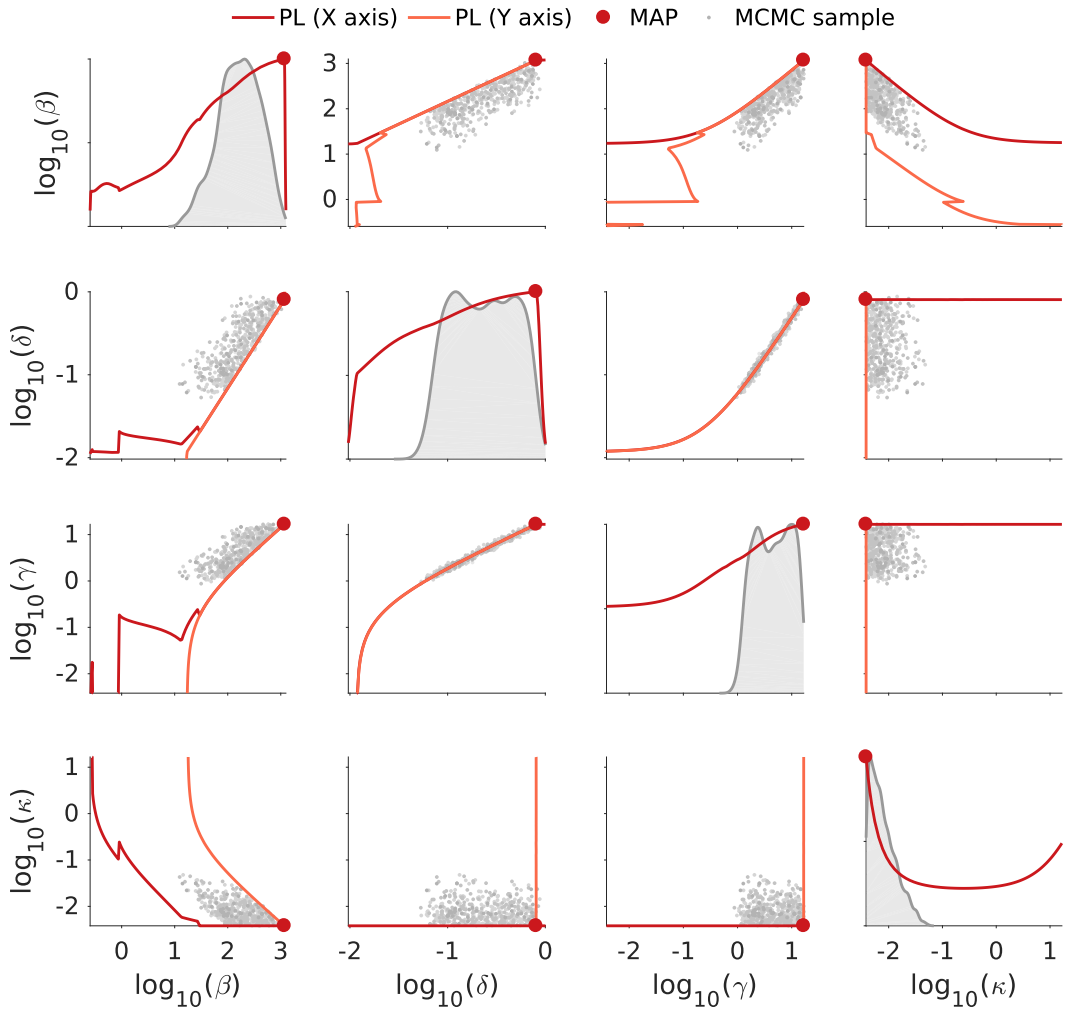

Figure S7: **Parameter correlations for model O1.** Related to Figure 2A in the main manuscript. The scatter plot matrix for the MCMC samples are depicted. The maximum a posterior estimate (MAP) and the profile likelihoods with respect to the parameter in the x-axis and y-axis are indicated. Individual parameter marginal distributions and profile likelihoods are shown on the diagonal.

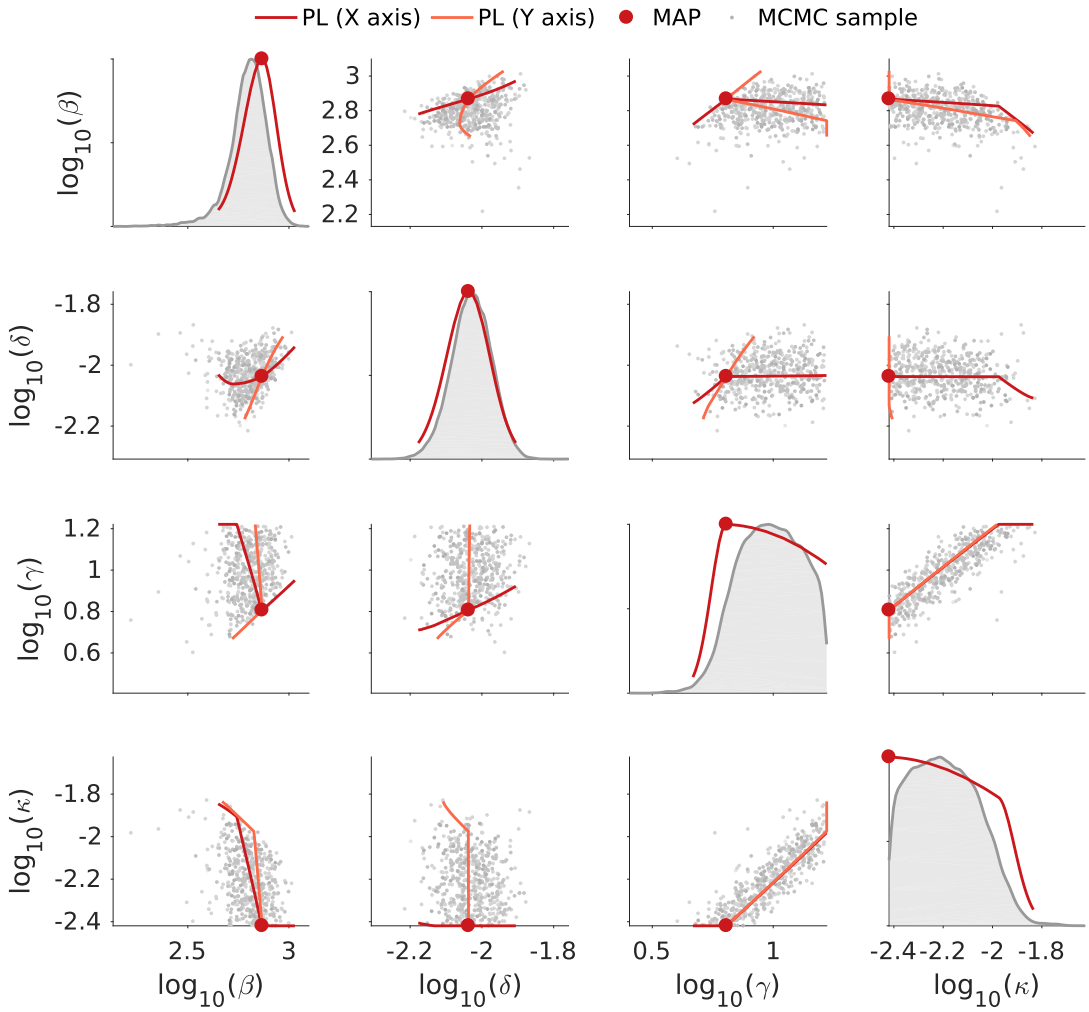

Figure S8: **Parameter correlations for model O2.** Related to Figure 2B in the main manuscript. The scatter plot matrix for the MCMC samples are depicted. The maximum a posterior estimate (MAP) and the profile likelihoods with respect to the parameter in the x-axis and y-axis are indicated. Individual parameter marginal distributions and profile likelihoods are shown on the diagonal.

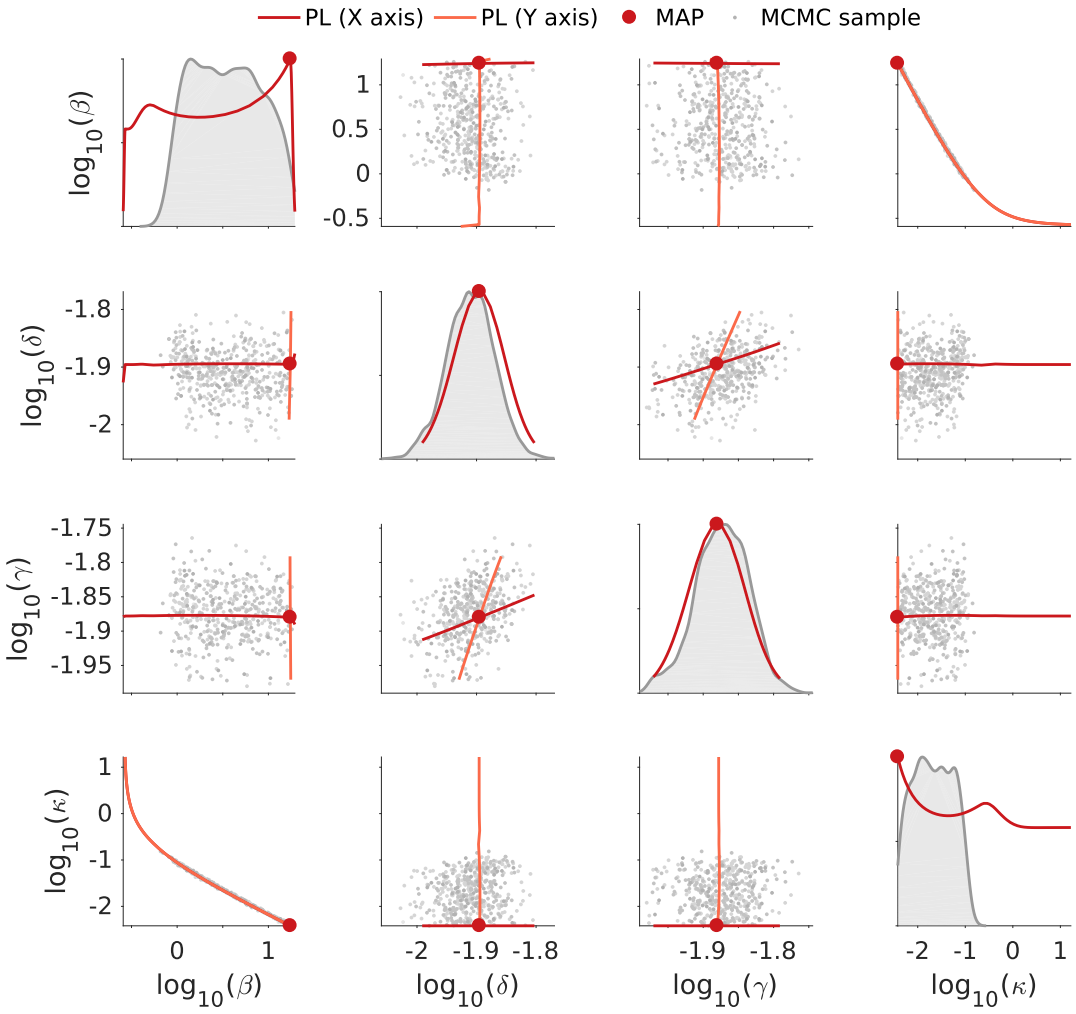

Figure S9: **Parameter correlations for model O3.** Related to Figure 2C in the main manuscript. The scatter plot matrix for the MCMC samples are depicted. The maximum a posterior estimate (MAP) and the profile likelihoods with respect to the parameter in the x-axis and y-axis are indicated. Individual parameter marginal distributions and profile likelihoods are shown on the diagonal.

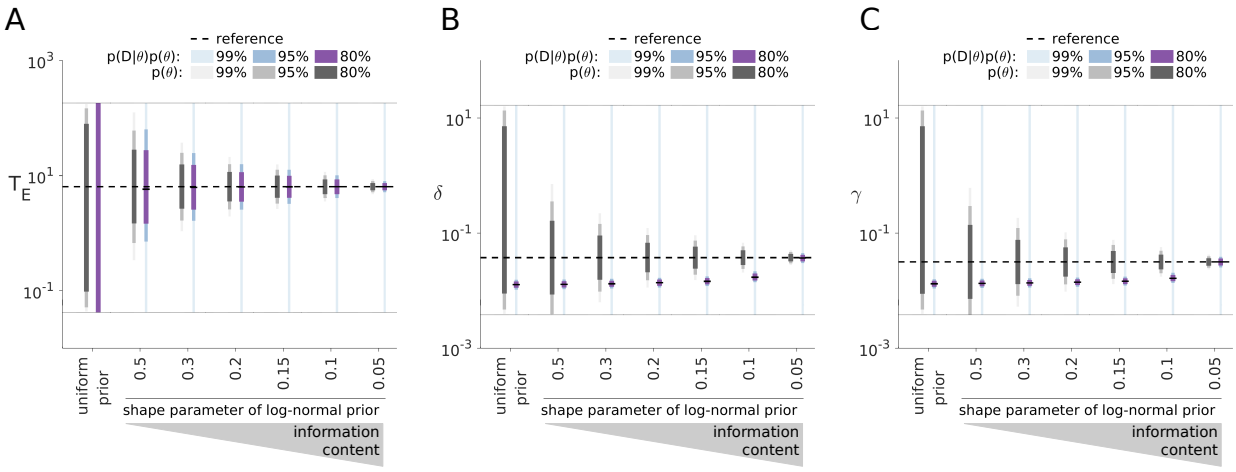

Figure S10: **Impact of the prior scale.** Parameter confidence intervals for a range of increasing prior scales for (A) the incubation time T_E, (B) the death rate δ, (C), and the recovery rate γ. The prior distributions $p(\theta)$ are depicted in grey and the approximated posterior $p(D|\theta)p(\theta)$ in purple.

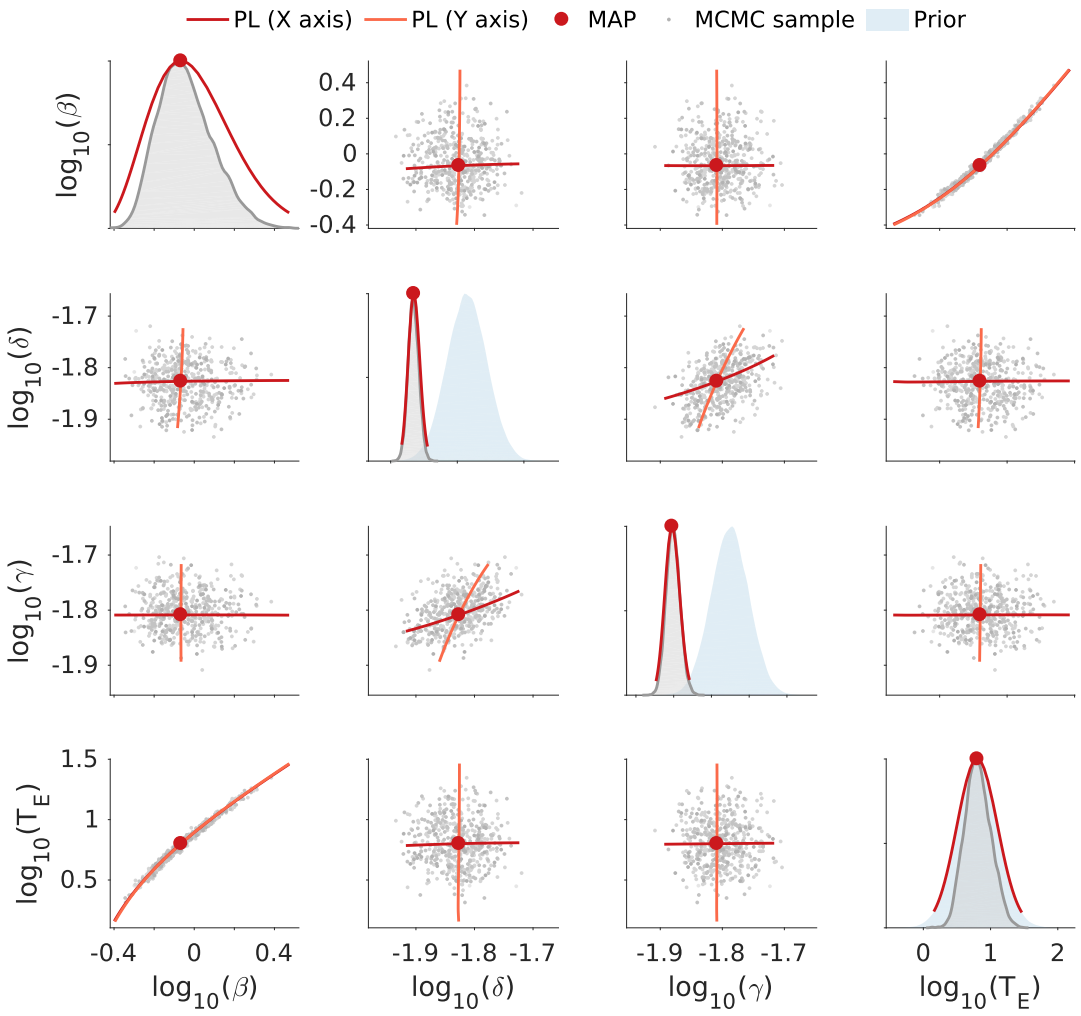

Figure S11: **Parameter correlations for model M1.** Related to Figure 4A in the main manuscript. The scatter plot matrix for the MCMC samples are depicted. The maximum a posterior estimate (MAP) and the profile likelihoods with respect to the parameter on the x-axis and y-axis are indicated. Individual parameter marginal distributions and profile likelihoods are shown on the diagonal. Parameter prior distributions are indicated in blue.

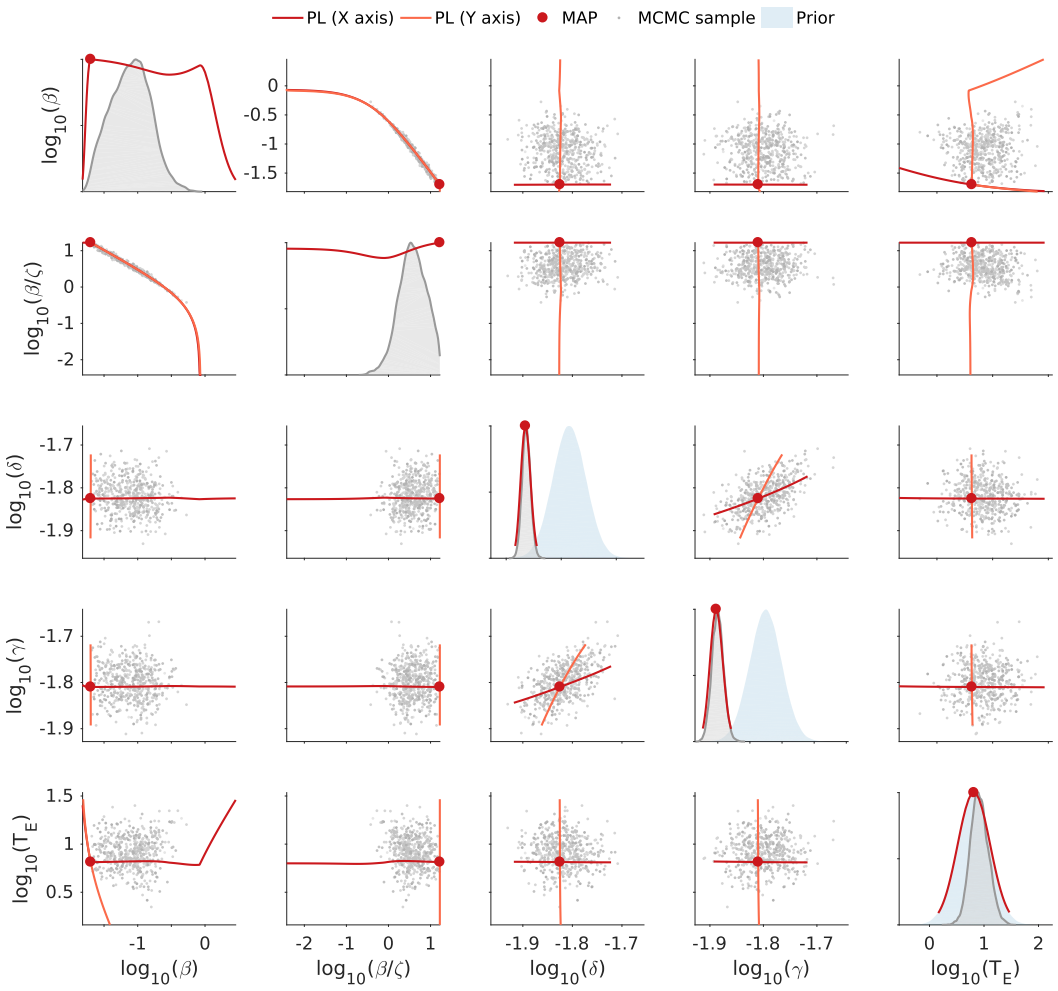

Figure S12: **Parameter correlations for model M2.** Related to Figure 4B in the main manuscript. The scatter plot matrix for the MCMC samples are depicted. The maximum a posterior estimate (MAP) and the profile likelihoods with respect to the parameter on the x-axis and y-axis are indicated. Individual parameter marginal distributions and profile likelihoods are shown on the diagonal. Parameter prior distributions are indicated in blue.

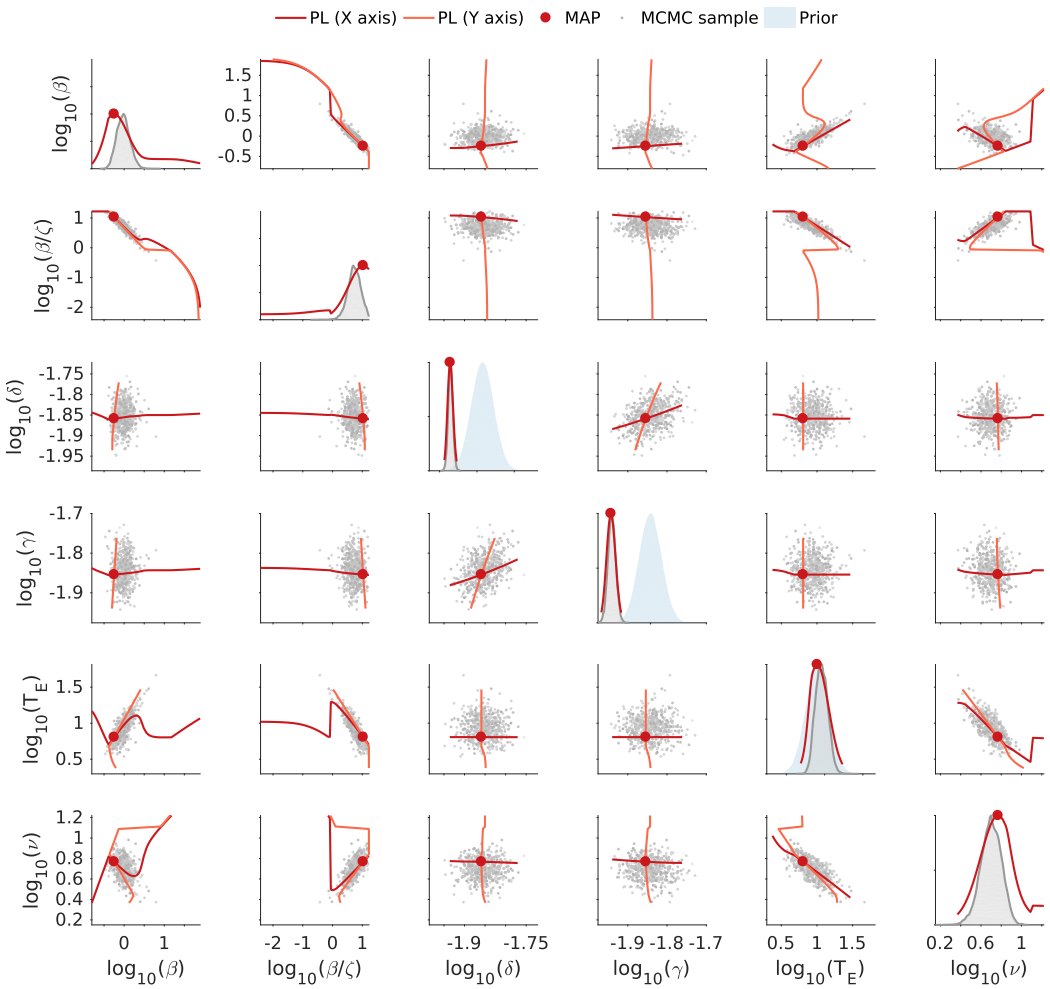

Figure S13: **Parameter correlations for model M3.** Related to Figure 4C in the main manuscript. The scatter plot matrix for the MCMC samples are depicted. The maximum a posterior estimate (MAP) and the profile likelihoods with respect to the parameter on the x-axis and y-axis are indicated. Individual parameter marginal distributions and profile likelihoods are shown on the diagonal. Parameter prior distributions are indicated in blue.

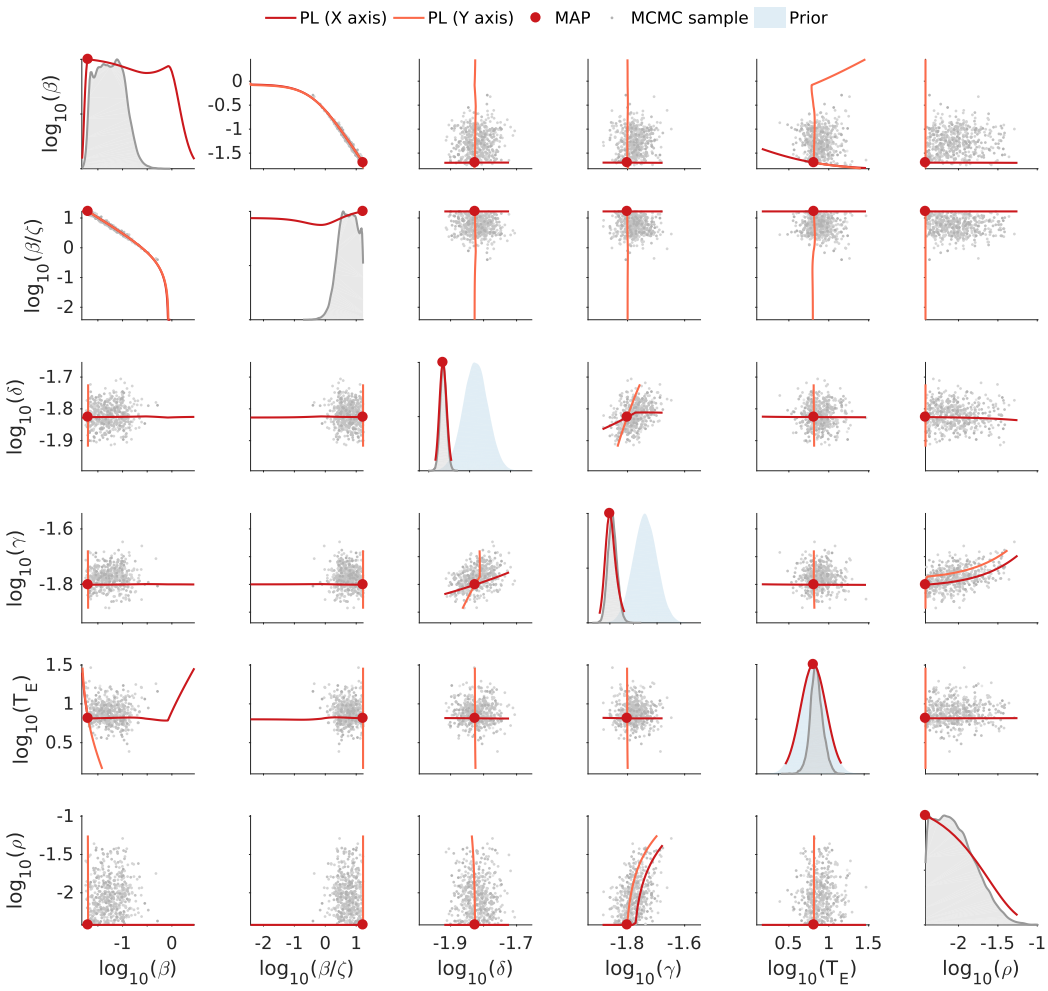

Figure S14: **Parameter correlations for model M4.** Related to Figure 4D in the main manuscript. The scatter plot matrix for the MCMC samples are depicted. The maximum a posterior estimate (MAP) and the profile likelihoods with respect to the parameter on the x-axis and y-axis are indicated. Individual parameter marginal distributions and profile likelihoods are shown on the diagonal. Parameter prior distributions are indicated in blue.

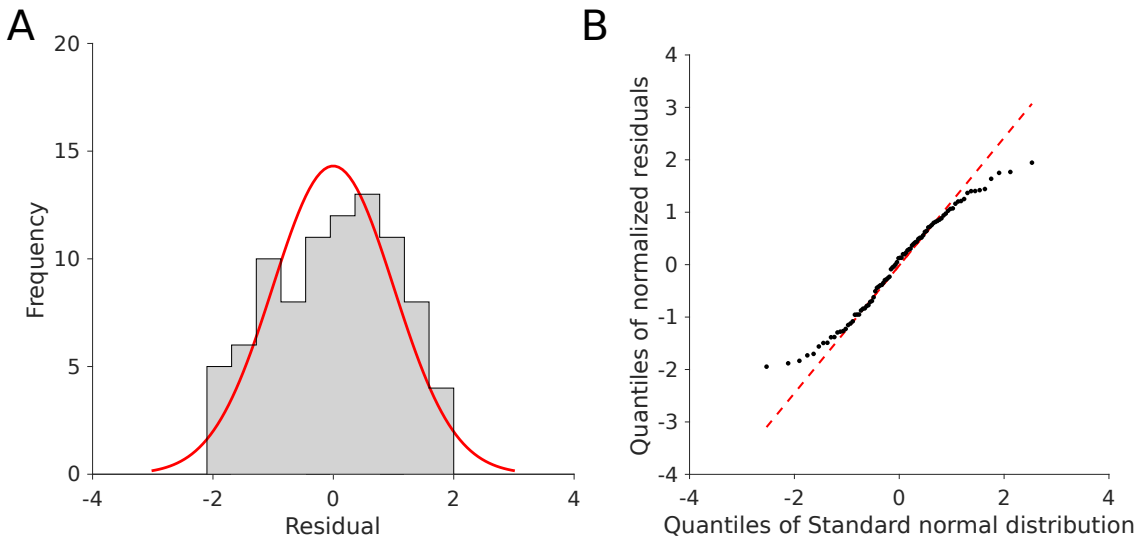

Figure S15: **Evaluation of residual distributions for the optimal model.** Related to Figure 7 in the main manuscript. (A) Distributions of the residuals $(\log \bar{y}_{i,k} - \log y_i(t_k))/\sigma_i$ for all observables and time points under the assumption of log-normally distributed measurement noise. The histogram indicates the empirical frequency of observations and the red line the theoretical limit distribution. (B) Normal QQ-plot for standardized residuals.

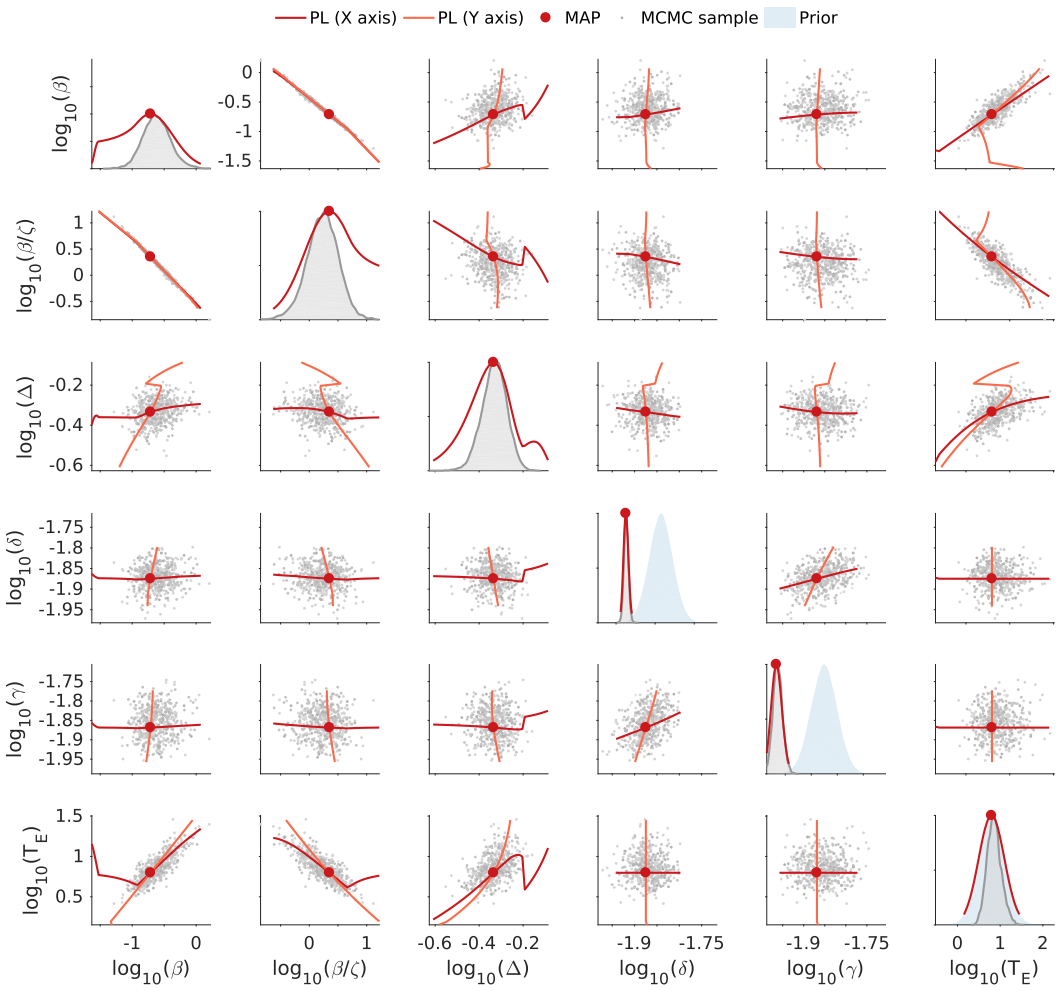

Figure S16: **Parameter correlations for model M2 with discrete intervention.** Related to Figure 7C in the main manuscript. The scatter plot matrix for the MCMC samples are depicted. The maximum a posterior estimate (MAP) and the profile likelihoods with respect to the parameter on the x-axis and y-axis are indicated. Individual parameter marginal distributions and profile likelihoods are shown on the diagonal. Parameter prior distributions are indicated in blue.